

# VLBI observations of 6.7 and 12.2 GHz methanol masers toward high mass star-forming regions

## II. Tracing massive protostars

V. Minier, J. E. Conway, and R. S. Booth

Onsala Space Observatory, 439 92 Onsala, Sweden

Received 20 November 2000 / Accepted 22 January 2001

**Abstract.** We compare the absolute positions of methanol maser sites with those of typical tracers of young massive stellar objects, such as ultra-compact H II regions, outflows and hot molecular cores. We have selected thirteen star-forming regions for which we have produced VLBI maps of 6.7 and 12.2 GHz methanol masers, and for which complementary high resolution images are available in the literature. These sources are namely: IRAS 20126+4104, NGC 7538, S 252, G 31.28+0.06, W 75N, S 255, S 269, Mon R2, G 9.62+0.20, Cep A, W 51, G 59.78+0.06 and G 29.95-0.02. Eight of the methanol maser sources coincide in position within 2000 AU with outflows and/or hot molecular cores, i.e. phenomena occurring at the earliest stage of massive star formation. Only two sources coincide in position with hyper-compact H II regions. We conclude that 6.7 and 12.2 GHz methanol masers are likely to be one of the first signposts of massive star formation and perhaps the first signpost of a massive protostar.

**Key words.** H II regions – masers – stars: formation – circumstellar matter – techniques: interferometric

### 1. Introduction

The earliest targeted surveys using single dish observations (Menten 1991; Caswell et al. 1995) toward star-forming regions suggested a close association between the 6.7 and 12.2 GHz methanol masers and the typical signposts of massive star formation such as ultra-compact H II regions (UC H II regions), OH and H<sub>2</sub>O masers. However, the unbiased Mount Pleasant survey of the Galactic plane, conducted from Tasmania (Australia), has shown that more than 50% of the new 6.7 GHz maser detections do not have any IRAS counterpart satisfying the UC H II region criteria (Ellingsen 1996a). Moreover, a recent targeted survey toward UC H II candidates, i.e. IRAS colour selected sources (see Wood & Churchwell 1989), shows a relatively poor detection rate (13%) of 6.7 GHz methanol masers (Szymczak et al. 2000). Similarly, Parkes-64 m observations toward 535 IRAS selected sources (i.e. UC H II region candidates) showed that only 37% of the UC H II region candidates exhibit methanol masers (Walsh et al. 1997). These results, from low resolution observations, indicate that the majority of the observed 6.7 and 12.2 GHz methanol masers are indeed not commonly associated with

UC H II regions, and conversely that only a small fraction of UC H II regions exhibit detectable methanol masers.

Furthermore, ATCA observations of both UC H II regions and 6.7 GHz methanol masers in the same site have revealed that in many sources the masers are not superimposed on the UC H II region (Walsh et al. 1998; Phillips et al. 1998; Ellingsen et al. 1996b). Instead, the masers are found offset from the UC H II region in many cases. In summary, the 6.7 GHz maser sites and probably their 12.2 GHz counterparts are not necessarily coincident with UC H II regions, even when their positions agree at single dish resolution. We might then ask: what is the relationship between methanol masers and massive star formation.

One possible scenario is that the 6.7 GHz methanol masers are associated with early phases of massive star formation, i.e. before the compact H II regions form, and then they are rapidly destroyed as the detectable UC H II region evolves (Walsh et al. 1998, 1999). In such a case, the methanol masers would be precursors of UC H II regions and might be associated with hot molecular cores. Masers would be detected toward UC H II regions in only a few cases. Such an association between hot cores and masers appears to hold for H<sub>2</sub>O masers (Codella et al. 1997). An alternative explanation is that the majority of methanol

---

Send offprint requests to: V. Minier,  
e-mail: [vincent@oso.chalmers.se](mailto:vincent@oso.chalmers.se)

masers are associated with lower mass protostars which do not have any UC H II region (Phillips et al. 1998).

The Onsala VLBI group has been conducting an extensive study of the Northern hemisphere methanol masers using the European VLBI Network (EVN) and the VLBA since early 1997 (Minier et al. 1998, 1999, 2000). In parallel, a blind survey of the Galactic plane has been undertaken in order to discover new 6.7 GHz methanol masers using the Onsala-25 m antenna. In Minier et al. (2000, hereafter Paper I), we presented the VLBI observations of 6.7 and 12.2 GHz methanol masers toward fourteen well known star-forming regions. The overall morphologies of the maser sites were described in Paper I. In many cases, the maser components delineate linear structures in the VLBI maps and exhibit linear velocity gradients consistent with rotating disks seen edge-on.

In the present paper, we investigate the nature of the association of the methanol masers with regions of massive star formation. Unlike the Southern hemisphere sites of methanol masers, the Northern star-forming regions exhibiting such masers have been extensively studied at other wavelengths using high resolution ( $<2''$ ) techniques. By comparing all the high resolution images of selected sources with the VLBI maps of the associated methanol masers, it should be possible to better understand the role of these masers in the evolution of young massive stellar objects. The first aim of this work is to identify the stellar objects traced by methanol masers. The mean separation between stellar objects in a cluster is about 0.1 pc (or  $\sim 2 \cdot 10^4$  AU) or 20 arcsec at 1 kpc (Lada et al. 1999). Therefore, different emissions from tracers detected within  $\sim 2$  arcsec should probably arise from the same star or protostar. The secondary purpose of the present study is to see how different species are geometrically related in star-forming regions. Thus, we have selected thirteen methanol maser sources, twelve from Paper I, for which accurate absolute positions are known, and for which detailed observations at other frequencies are available in the literature. W 48 and S 231 in Paper I are not included in the source sample. The absolute position of W 48 is known only within  $\sim 30$  arcsec while S 231 is a poorly imaged region at high resolution. A new source has been added to the original sample of maser sites: IRAS 20126+4104. Thus, the thirteen selected maser sources are: IRAS 20126+4104, NGC 7538, S 252, G 31.28+0.06, W 75N, S 255, S 269, Mon R2, G 9.62+0.20, Cep A, W 51, G 59.78+0.06 and G 29.95-0.02.

## 2. Observations and data analysis

### 2.1. VLBI observations

The 6.7 GHz EVN observations were conducted in May 1997, November 1998 and November 1999. The VLBA observations at 12.2 GHz were conducted in July 1997, November 1998, and January 1999. The EVN observations in November 1999 were similar to those in November

1998. One new source, observed during that EVN session, is included in our sample: IRAS 20126+4104. The observations as well as the data analysis are fully described in Paper I. Standard amplitude, delay, rate and phase-referenced calibration and imaging procedures to analyse spectral line VLBI data were used. For this new source, the cross power spectrum (scalar averaging) taken on the baseline Effelsberg-Onsala as well as the EVN map of the maser components are presented in Fig. 1.

We were able to find the absolute positions for seven sources by applying standard imaging techniques (AIPS tasks IMAGR and JMFIT) to the data and phase referencing to a close calibrator source (Table 1). The estimated error on the absolute position is  $\sim 30$  mas. We could not find the absolute position of six sources because the data were not phase referenced or because the continuum emission used for phase referencing was too weak to allow proper phase calibration.

### 2.2. Reliability of the ATCA observations

For the sources for which no VLBI position has been derived, ATCA positions are taken (Table 1). We can estimate the accuracy of the ATCA positions by considering several sources observed both by the ATCA and the VLBA.

G 59.78+0.06 was observed at 6.7 GHz using the ATCA (Phillips, priv. comm.) and at 12.2 GHz using the VLBA (Paper I), respectively. The absolute positions of the peak at  $17 \text{ km s}^{-1}$  seen in both of the 6.7 and 12.2 GHz spectra coincide within 400 mas, respectively  $\text{RA} = 19^{\text{h}}43^{\text{m}}11^{\text{s}}.207$ ,  $\text{Dec} = 23^{\circ}44'02.57''$  and  $\text{RA} = 19^{\text{h}}43^{\text{m}}11^{\text{s}}.198$ ,  $\text{Dec} = 23^{\circ}44'02.98''$ . Two other sources, G 9.62+0.20 and W 51, were also observed at both frequencies using the ATCA (Phillips et al. 1998; Caswell, priv. comm.) and the VLBA. The absolute coordinates of the 12.2 GHz methanol masers in G 9.62+0.20 were not given in Paper I while the J2000 positions of the 12.2 GHz masers in W 51 were wrong. The data have been reprocessed and the accurate VLBA positions of these two sources agree within less than 300 mas with the ATCA positions. This demonstrates that the ATCA positions are reliable at subarcsecond levels, even for declinations greater than  $10^{\circ}$ . This result also suggests that 6.7 and 12.2 GHz masers with the same velocity occur at the same location.

## 3. Comments on individual sources

In this section, we describe the environment of each of the thirteen selected sources, and we compare the positions of methanol masers with those of typical tracers of massive star formation.

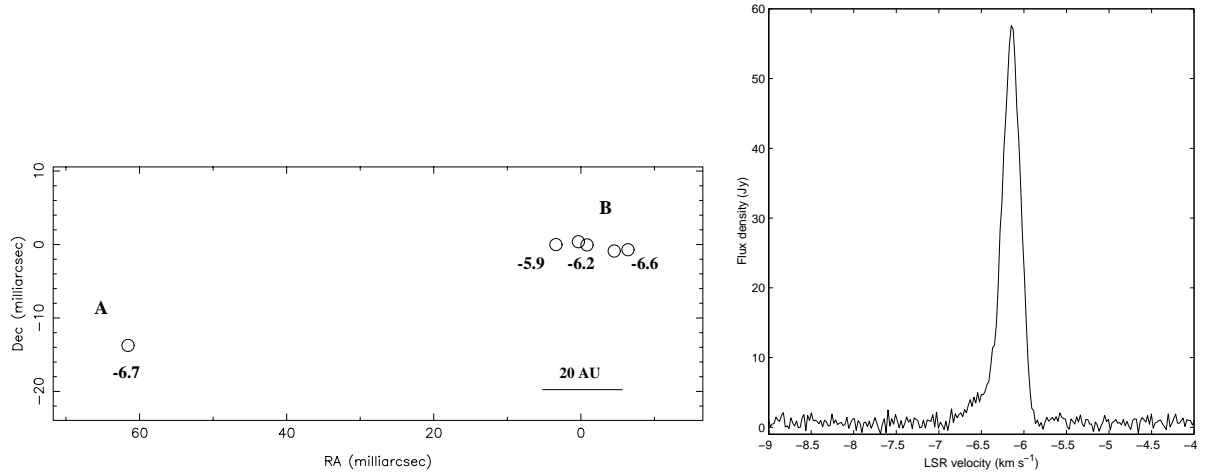


**Fig. 1.** IRAS 20126+4104: Map of 6.7 GHz (circles) methanol masers with the indicated values of LSR velocities and maser spectrum at 6.7 GHz taken on the Onsala-Effelsberg baseline

**Table 1.** Absolute positions of the methanol maser sites. The coordinates are either from our VLBI observations presented in Paper I and in this paper, or are the ATCA positions taken from Phillips (priv. comm.) and Walsh et al. (1998)

Source name	Array	Coordinates (J2000)		$V_{\text{peak}}$ km s <sup>-1</sup>
		RA(h m s)	Dec( ° ' ")	
IRAS 20126+4104	EVN	20:14:26.044	41:13:33.39	-6.2
NGC 7538	VLBA	23:13:45.364	61:28:10.55	-56.2
AFGL 5180(S 252)	ATCA	06:08:53.346	21:38:28.67	10.6
G 31.28+0.06	ATCA	18:48:12.385	-01:26:22.60	110
W 75N	ATCA	20:38:36.452	42:37:36.07	6.8
S 255	ATCA	06:12:54.024	17:59:23.01	4.7
S 269	ATCA	06:14:37.055	13:49:37.15	15.2
Mon R2	ATCA	06:07:47.867	-06:22:56.89	11
G 9.62+0.20	VLBA	18:06:14.659	-20:31:31.57	1.3
Cep A	VLBA	22:56:18.095	62:01:49.45	-4.2
W 51	VLBA	19:23:39.821	14:31:04.47	56.1
G 59.78+0.06	VLBA	19:43:11.248	23:44:03.34	26.9
G 29.95-0.02	VLBA	18:46:03.741	-02:39:21.43	96.8

### 3.1. Tracers of massive star formation

For this work, the most common tracers were selected. In rough order of ages, they are:

1. *Hot molecular cores* are the sites where high mass stars are born. They are usually found near UC H II regions and are coincident with H<sub>2</sub>O masers. They mark a stage of high mass star formation prior to the UC H II phase. The rich chemistry in these hot ( $\sim 200$  K), dense ( $>10^7$  cm<sup>-3</sup>) and small ( $\sim 0.5$  pc or  $10^5$  AU) cores leads to abundant formation of NH<sub>3</sub>, CH<sub>3</sub>OH, CH<sub>3</sub>CN and more complex organic molecules, making them natural tracers of high density (Kurtz et al. 2000). Furthermore, the temperature profiles measured by Cesaroni et al. (1998) toward three hot cores are well modelled using a disk-like geometry;
2. *Bipolar outflows and jets* are frequently found associated with sites of star formation. The outflows are believed to be characteristic of newly formed stars. They are often more massive than the mass of the central protostar and the origin of these high masses are still unclear. Many scenarios have been suggested in order to explain the formation of bipolar outflows, such as outflows driven by winds from the accretion disk surface, bipolar jet entraining the surrounding ISM, or ISM swept-up by protostellar winds (see Churchwell 1999; Bachiller & Tafalla 1999; Shu et al. 1991). The outflows have multiple observational manifestations. The high velocity outflows can be observed directly with CO lines. In addition, the interaction of the high velocity jets from the protostars with the surrounding environment produces shocked regions that are

detected using molecular tracers (e.g SiO, HCO<sup>+</sup>, and H<sub>2</sub> at 2  $\mu$ m) and probably interstellar masers (e.g OH, H<sub>2</sub>O and NH<sub>3</sub> masers). They are also delineated by elongated radio continuum emission and appear as ionised stellar outflows (e.g CepA in Rodríguez et al. 1994). The outflows extend up to a few pc ( $\sim 2 \cdot 10^5$  AU);

3. *Ultra Compact H II regions* are the manifestations of young massive stars. The massive stellar object, still embedded in its natal cocoon of dust and molecular gas, emits strong ultraviolet radiation that ionises the surrounding environment. The UC H II regions have sizes smaller than 0.1 pc ( $\sim 2 \cdot 10^4$  AU). The spectra of these ionised regions are dominated by free-free emission at cm wavelengths and by thermal dust emission for wavelengths below 3 mm. The UC H II regions are the most luminous objects in the Galaxy observed at 100  $\mu$ m and they also emit strong radio continuum at 5, 15 and 22 GHz observable at high resolution using the VLA (e.g Kurtz et al. 1994).

VLBI observations offer a resolution of a few mas and absolute positions with errors less than 50 mas. ATCA positions are accurate to 1 or 2 arcsec. By comparing the position of the methanol masers with the position of tracers of massive star formation observed at high resolution, it is possible to see if the methanol masers coincide with massive young stellar objects. For example, the radio continuum emission from UC H II regions usually has positions determined within errors of less than 1 arcsec. Similarly, hot molecular cores, which are believed to represent earlier stages of massive star formation (Kurtz et al. 2000), are detected using tracers like NH<sub>3</sub> and CH<sub>3</sub>CN. Such species are observed using connected element interferometers such as VLA and IRAM-Plateau de Bure. Therefore they also have positions known to better than 1 arcsec. Since 2 arcsec is  $\sim 2000$  AU at 1 kpc, which is smaller than the mean distance between stellar objects in a cluster, we will consider as spatially coincident and arising from the same star or protostar, different tracers falling within  $\sim 2$  arcsec and having similar LSR velocities (if available).

Detailed comments on the nature of each methanol maser site as well as a schematic illustration or an image of the star-forming regions showing different tracers for some sources of interest, are given in the text below.

### 3.2. IRAS 20126+4104

IRAS 20126+4104 is a very young and massive protostar embedded in a dense and hot molecular core (Fig. 2). It lies at the centre of a rotating and slightly collapsing disk. It also powers a bipolar jet and outflow perpendicular to the CH<sub>3</sub>CN and NH<sub>3</sub> disk (Cesaroni et al. 1997, 1999). The 6.7 GHz methanol masers coincide in position with the hot molecular core. However, they do not lie on the peak of CH<sub>3</sub>CN core emission, but they are offset from the centre of the disk by 1200 AU, assuming a distance of 1.7 kpc from the sun (Fig. 2). Since the methanol maser

positions are from EVN measurements and the position of the hot core is known within 300 mas or 510 AU, this positional offset may be significant. Recent modelling of the H<sub>2</sub>O maser morphology at the root of a bipolar jet, shows that the centre of the jet is located 200 mas SE from the CH<sub>3</sub>CN emission peak (Moscadelli et al. 2000), making the methanol masers even more offset from the protostar. The methanol masers are possibly located in the interface between the NH<sub>3</sub> disk and the HCO<sup>+</sup> outflow (Fig. 2). Their detailed morphology is *simple* (according to the nomenclature in Paper I) corresponding to a spectral feature of  $\sim 1$  km s<sup>-1</sup> linewidth (Fig. 1). Two maser clumps (A and B in Fig. 1) are separated by 100 AU. Unlike other masers in Paper I, the masers do not delineate any disk-like structure.

### 3.3. NGC 7538

The methanol masers in NGC 7538-IRS 1 (Fig. 3) coincide in position with the radio-continuum and with the H66 $\alpha$  recombination line emission observed by Gaume et al. (1995). The radio continuum emission is elongated north-south and contains two radio lobes (northern and southern cores) and a so-called spherical component located south of the double core structure. The groups of methanol masers identified in Paper I coincide with radio continuum features. For instance, maser group C coincides with the southern core while E form a circular structure near the spherical component. Gaume et al. (1995) resolved the compact double core into many bright clumps, and interpreted the radio emission morphology as created by an ionised stellar wind outflow.

### 3.4. AFGL 5180 (S 252 in Paper I)

The methanol masers in AFGL 5180 (labelled S 252 in Menten 1991) are associated with the luminous far infrared source, IRAS 06058+2138, and with an ammonia core (Davis et al. 1998). The masers are not coincident with the infrared source itself, but they are instead located at the neck of the infrared nebula, at the position of the near infrared source NIRS 1 (Tamura et al. 1991) that is believed to power an outflow. The mean LSR velocity of the methanol masers does not correspond with that of the CO line tracing the outflows (Snell et al. 1988). The position angle (PA) of the bipolar outflow is 130° while the PA of the line of masers is 70°.

### 3.5. G 31.28+0.06

The 6.7 GHz methanol maser source does not coincide with the UC H II region G 31.28+0.06. The maser site is offset by 6.3 arcsec from the ionised region (Walsh et al. 1998), i.e. offset by  $3.5 \cdot 10^4$  AU at a distance of 5.6 kpc (Kurtz et al. 1994). There is no reported molecular or IR emission associated with the maser site.

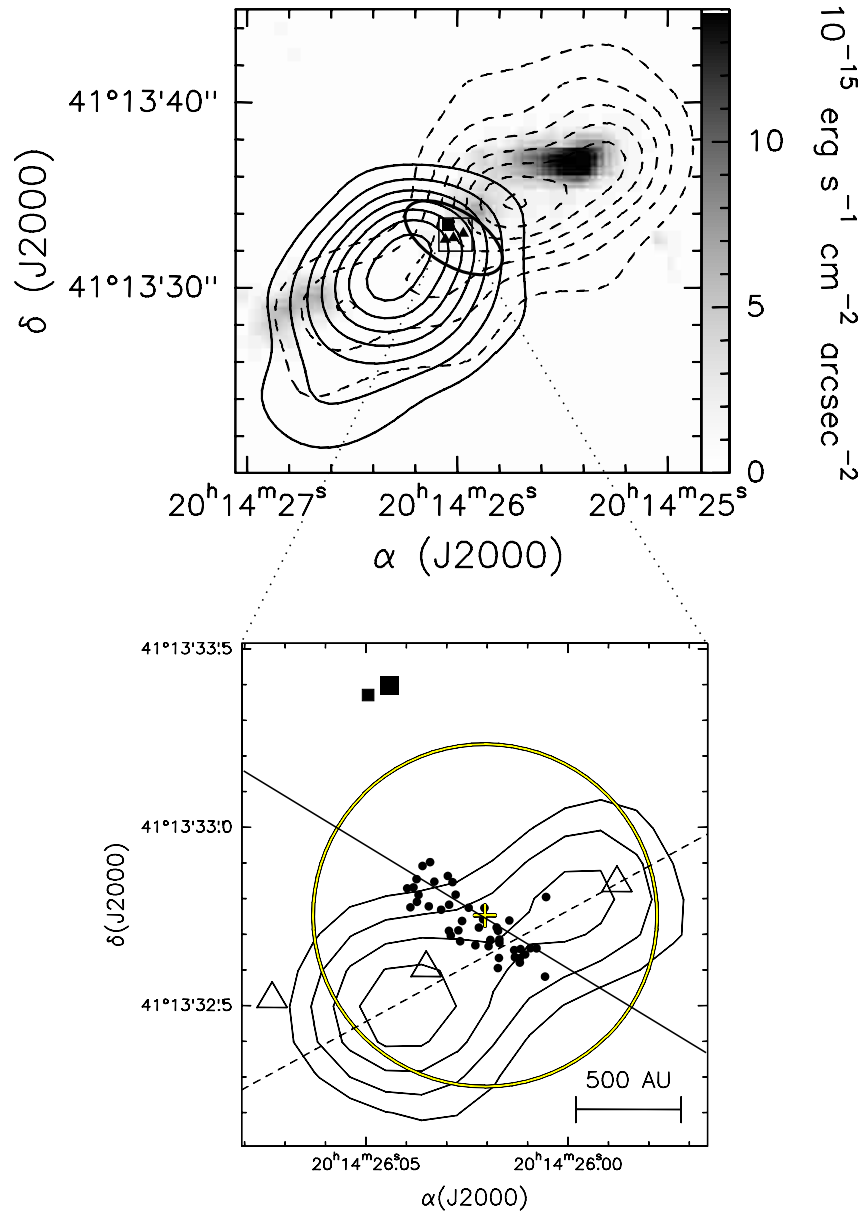


**Fig. 2.** Different tracers of the massive protostar in IRAS 20126+4104. Top: contours represent the blue (continuous line) and redshifted (dashed line) component of the  $\text{HCO}^+$  outflow. The grey scale represents the  $\text{H}_2$  emission. The  $\text{H}_2\text{O}$  (triangles) and  $\text{CH}_3\text{OH}$  (squares) masers are seen projected onto the  $\text{NH}_3$  disk (black ellipse). Bottom: close-up of the inner region of the hot core. The large circle represents the total extent of the 3 mm emission centred on the cross. The contours are the radio continuum emission at 3.6 cm that is believed to trace a bipolar jet (dashed line) roughly perpendicular to the major axis (solid line) of the disk traced by  $\text{CH}_3\text{CN}$  (black dots) (Cesaroni et al. 1997; Zhang et al. 1998b; Hofner et al. 1999; Moscadelli et al. 2000. Figures courtesy of Riccardo Cesaroni). The methanol masers lie offset from the centre of the hot core while the  $\text{H}_2\text{O}$  masers delineate the root of the bipolar jet

### 3.6. W 75N

The methanol masers lie at less than 2 arcsec to the NE of the radio continuum emission VLA 1 (Fig. 4) that is believed to power an ionised stellar wind outflow (Torrelles et al. 1997). The elongated morphology of the continuum emission with a position angle of  $43^{\circ}$  follows the linear morphologies of the OH and  $\text{H}_2\text{O}$  masers (Torrelles et al. 1997). The line of methanol masers coincides in space and in velocity with the northern part of the OH maser line,

and has a PA of  $42^{\circ}$  (Fig. 4). The methanol masers are blueshifted with respect to the  $\text{H}_2\text{O}$  masers. The mean velocity of the methanol masers is  $5 \text{ km s}^{-1}$  while the mean velocity of the  $\text{H}_2\text{O}$  masers and the ambient molecular cloud is  $10 \text{ km s}^{-1}$ . Note that the error on the declination of the maser site may be larger than 1 arcsec due to the low elevation of that source during the ATCA observations (Phillips, priv. comm.).

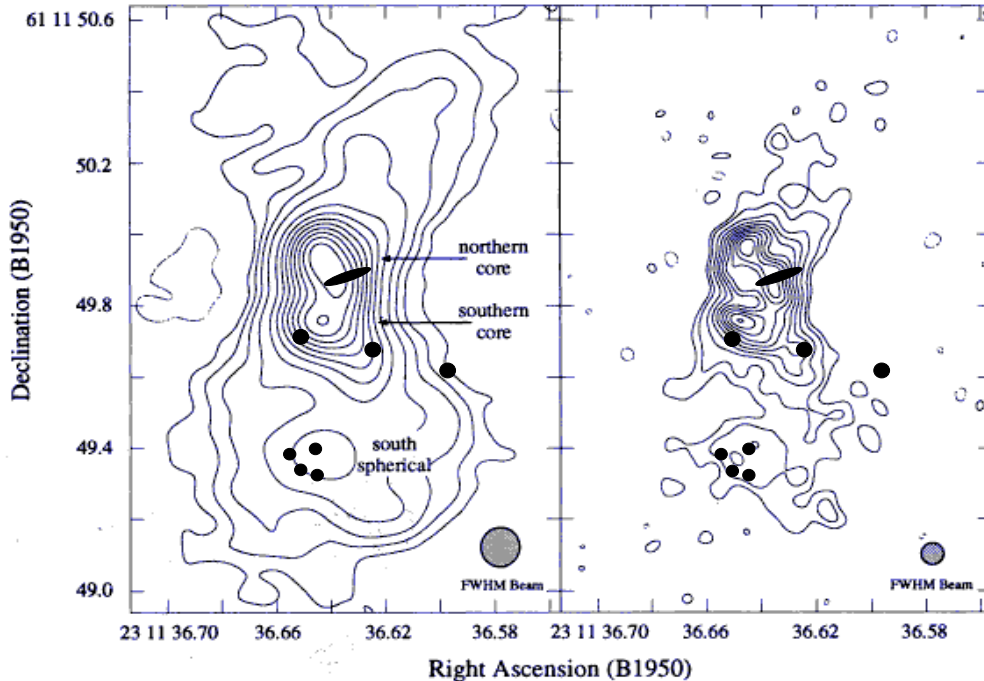


**Fig. 3.** NGC 7538-IRS 1. Contour maps of the naturally (left) and uniformly (right) weighted images of the 1.3 cm radio continuum taken from Gaume et al. (1995) (reproduced by permission of the AAS). The black symbols (circles and ellipse) mark the position of the 6.7 GHz methanol masers taken from Paper I. The right image has a higher resolution that identifies many clumps where the masers occur. The absolute position of the 1.3 cm image is known to an accuracy of 100 mas

### 3.7. S 255

The 6.7 GHz methanol masers (Fig. 5) coincide in position with the near infrared source NIRS 3 detected by Tamura et al. (1991). NIRS 3 is coincident with a weak radio source, S 255-2c and with the 20  $\mu\text{m}$  infrared source IRS 1 (Snell & Bally 1986) that may be a UC H II region. S 255-2c is located at  $\sim 1$  arcmin south from the UC H II region G 192.58-0.04. In addition, observations of  $\text{H}_2$  at 2  $\mu\text{m}$ , which is a good tracer of shocks at the termination of the high velocity outflows, have shown that NIRS 3 is powering an infrared jet of 1 pc extent with a PA of  $67^\circ$ , as well as a molecular outflow (Miralles et al. 1997).

### 3.8. S 269

No known tracer of a massive star is located at the position of the methanol masers. For instance, Kurtz et al. (1994) did not find any UC H II region toward S 269 despite the presence of an IRAS source satisfying the Wood & Churchwell criteria.

### 3.9. Mon R2

The 6.7 GHz methanol masers do not coincide with the radio continuum emission reported in Walsh et al. (1998). The maser site is offset by 15 arcsec from the UC H II region, i.e. offset by  $1.2 \cdot 10^4$  AU at a distance of 830 pc. The radio continuum peak emission coincides with that of the infrared source, IRS 3. This infrared source is resolved into three components (Koresko et al. 1993) and

shows evidence for a disk-like structure with a PA of  $140^\circ$  (Yao et al. 1997). The line of masers in Mon R2 has a PA of  $50^\circ$ , i.e. the maser line is perpendicular to the major axis of the infrared disk. Given the resolution of the infrared observations, it is however impossible to tell which resolved NIR source is related to the methanol maser site.

### 3.10. G 9.62+0.20

The 12.2 GHz methanol masers are projected onto the radio continuum component E in G 9.62+0.19 (Fig. 3 in Hofner et al. 1996). Observations of  $\text{CH}_3\text{CN}$ ,  $\text{NH}_3$ ,  $\text{C}^{18}\text{O}$  as well as mm and cm continuum observations have shown that E is a compact, dense and warm molecular core with an embedded UC H II region located near the edge of the molecular cloud core (Hofner et al. 1996).

### 3.11. Cep A

The 12.2 GHz methanol masers lie in the near environment of a radio continuum emission (Fig. 6) that traces a bipolar ionised outflow (Torrelles et al. 1996). The observed  $\text{H}_2\text{O}$  masers may trace a disk (Torrelles et al. 1996) and the OH masers may trace a shell around the radio continuum source (Migenes et al. 1992). Given their location, the methanol masers are likely part of the  $\text{H}_2\text{O}$  maser disk. They could be located at a radius of  $\sim 700$  AU in such a disk while the  $\text{H}_2\text{O}$  masers arise from regions at only 300 AU from the centre. The velocities of the methanol masers are between  $-4.2$  and  $-1.9 \text{ km s}^{-1}$  and hence, are

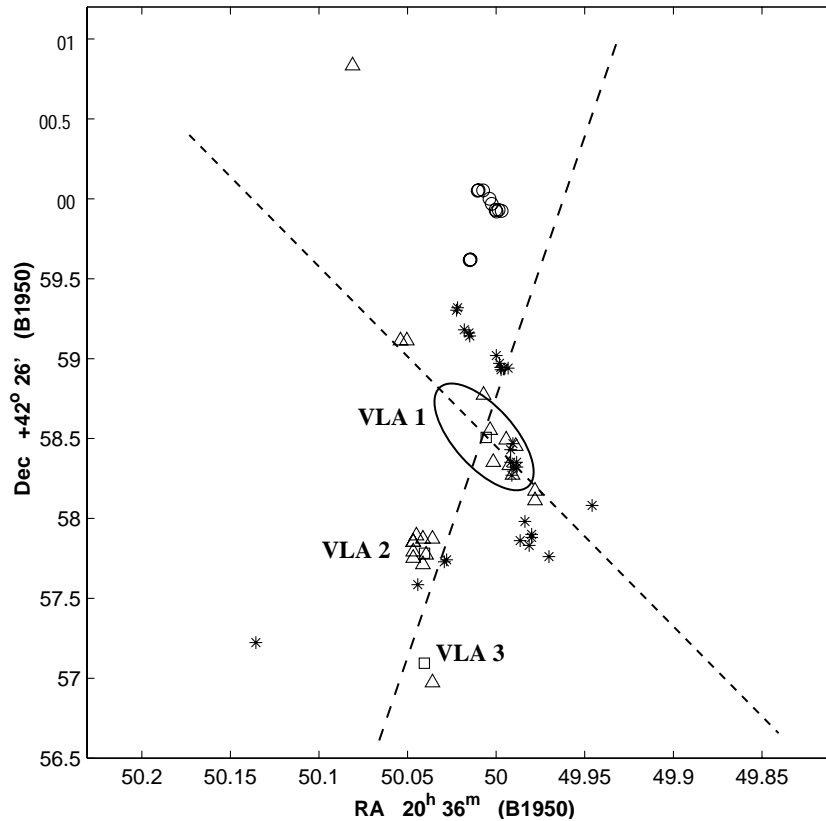


**Fig. 4.** Masers and radio jet in W 75N(B). The H<sub>2</sub>O (triangles), OH (stars), and 6.7 GHz CH<sub>3</sub>OH (circles) masers form an elongated structure oriented N–S. The three radio continuum sources VLA 1, VLA 2 and VLA 3 are marked by squares. The position angle and the dimensions of the thermal radio continuum jet from VLA 1 are indicated by the ellipse. The positions of the radio continuum VLA regions, H<sub>2</sub>O, OH masers are known to an accuracy of 100 to 300 mas while the error on absolute positions of the 6.7 GHz CH<sub>3</sub>OH masers is about 1 or 2 arcsec. Virtually all of the tracers lie within the dashed lines and all could be part of a bipolar conical structure

all redshifted with respect to the water masers which have a mean velocity of  $-11 \text{ km s}^{-1}$ . This latter velocity agrees with that of the ambient cloud.

### 3.12. W 51-North (G 49.49-0.37)

The 12.2 GHz methanol masers are coincident with the UC H II region D2 (Fig. 7) in W 51-North (Gaume et al. 1993). In that region, all the masers (H<sub>2</sub>O, OH, NH<sub>3</sub> and CH<sub>3</sub>OH) are aligned along an elongated structure traced by thermal NH<sub>3</sub> and CS emission (Zhang et al. 1995, 1998a). This structure has been interpreted as an outflow, but it is still not clear which source is powering that molecular outflow: the UC H II region W 51-D2 or the molecular core W 51-North:dust.

### 3.13. G 59.78+0.06

The methanol masers do not coincide with any tracer of massive star formation observed at high resolution. No radio continuum from a UC H II region was found toward that source (Kurtz et al. 1994) despite a detected infrared source satisfying the Wood & Churchwell criteria.

### 3.14. G 29.95-0.02

The 12.2 GHz methanol masers in G 29.96-0.02 arise from a linear structure offset from the UC H II region by  $2 \cdot 10^4 \text{ AU}$  (Fig. 8). They are clearly projected onto the hot core traced by the CH<sub>3</sub>CN and NH<sub>3</sub> emission, which is believed to represent a very early stage of massive star formation (Cesaroni et al. 1998).

## 4. Discussion

### 4.1. Methanol masers and massive star formation

In Sect. 3, we compared the absolute positions of the methanol maser sites with those of the tracers of massive star formation such as UC H II regions, bipolar outflows and hot cores. Thirteen sources were studied. Two sources coincide with UC H II regions (G 9.62+0.20 and W 51). Seven sources (IRAS 20126+4104, NGC 7538, AFGL 5180, W 75N, S 255, Cep A and W 51) are located at less than 2000 AU from outflows. Two sources (G 29.95-0.02 and IRAS 20126+4104) coincide with hot cores. Three sources (G 31.28+0.06, S 269 and G 59.78+0.06) do not coincide with any known UC H II region, outflow or hot core. For one source, Mon R2, it is not clear whether

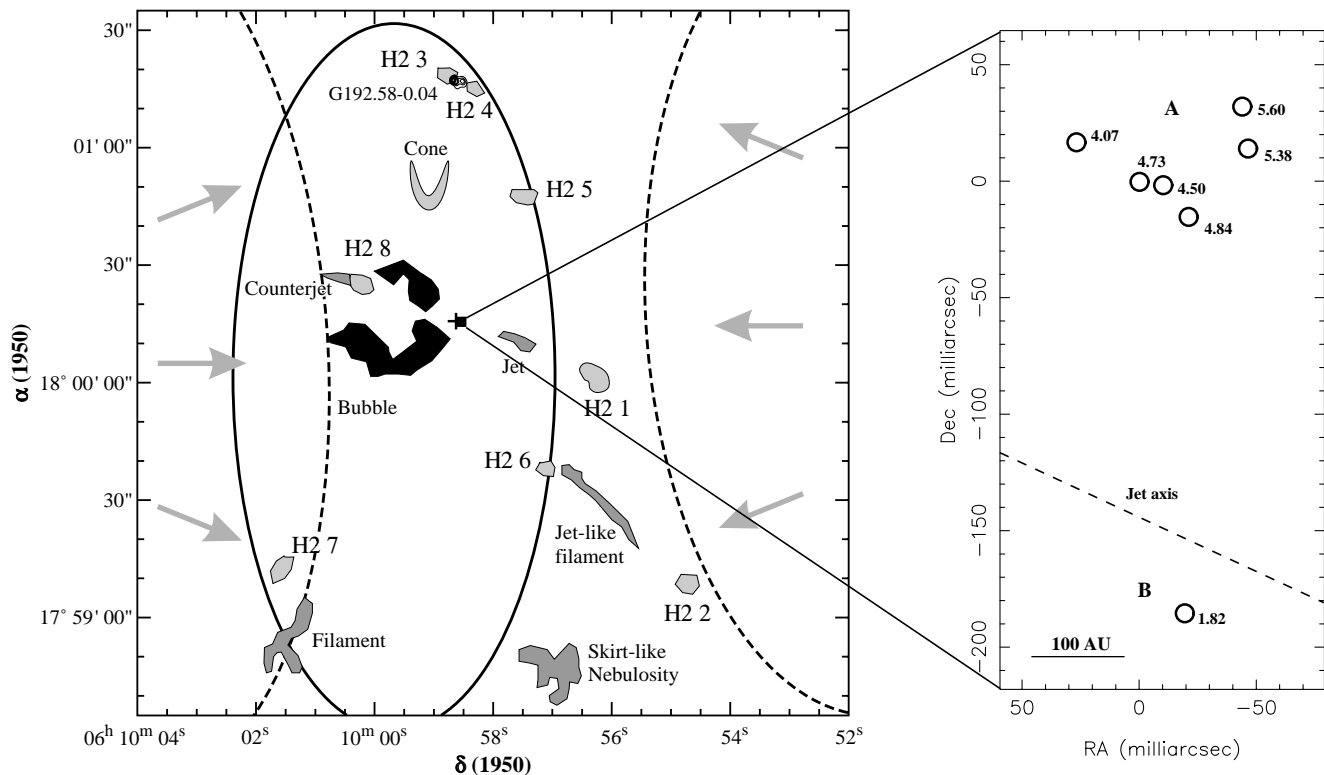


**Fig. 5.** Left: schematic diagram of S 255-IR, taken from Miralles et al. (1997) (reproduced by permission of the AAS). The large ellipse (solid line) delineates a region of a dense molecular core between two large optical H II regions S 255 and S 257 (dashed lines); H<sub>2</sub> objects are shown in light grey and the infrared source NIRS 3 by a cross. The black-shaded area represents the “bubble” of H<sub>2</sub> emission. The black square marks the position of the 6.7 GHz methanol masers coincident with NIRS 3. The masers are located at the centre of a bipolar jet. Right: close-up of the maser site. The values correspond to the LSR velocity of the maser components. The dashed line is the jet axis passing through NIRS 3 with a PA of 67°. The position of NIR 3 is known to an accuracy of 1 arcsec

the maser source coincides with the outer edge of a UC H II region or with another young massive star. The results are summarised in Table 2. Although in many cases the maser sites appeared (from single dish observations) to be associated with UC H II regions, high resolution imaging have shown that they do not coincide in position with them in eleven cases out of thirteen.

Outflows emerging from compact sources and hot molecular cores are believed to trace very early stages of massive star formation, often prior to the development of UC H II regions. The results of the comparison of the methanol maser absolute positions with the precise location of typical tracers of young massive stars have shown that the masers are seen at the positions of the markers of the earliest phases of star formation. Eight maser sites out of thirteen coincide within 1 arcsec with outflows and hot cores. Only two sources, G 9.62+0.20 and W 51, clearly coincide with a UC H II region. In both cases, the ionised regions have relatively small dimensions, and should be defined as hyper-compact H II regions. For example, the diameter of the hyper compact H II region in G9.62+0.20 is only  $\sim 600$  AU. The extreme compactness of these regions may be a sign of their youth. The absence of detected UC H II regions in most of methanol maser sources could mean that methanol masers trace nascent massive stars still

experiencing a massive infall that blocks the development of a UC H II region, i.e. protostellar objects. Our results confirm previous work by Walsh et al. (1998) who found that 80% of the methanol masers in their sample of 233 sources do not coincide with any UC H II region. Instead it was suggested that the masers are related to an earlier stage in the formation of massive stars. To summarise, assuming that methanol masers are always associated with a young massive stellar object, they are one of the first signposts of massive star formation.

#### 4.2. Methanol masers and NIR sources

In their near-infrared survey, Walsh et al. (1999) found that  $\sim 50\%$  of the methanol maser sites have a NIR counterpart. They argued that the NIR emission could mark the location of embedded massive stars in a pre-UC H II phase. However,  $\sim 60\%$  of the UC H II regions within their source sample are also associated with NIR sources. Similar observations of NIR emission associated with different stages of massive star formation have been made by Testi et al. (1998) in their study of G 9.62+0.20. Testi et al. have shown that detectable NIR emission could be produced at the earliest stage of massive star formation. According to their modelling of the infrared emission from

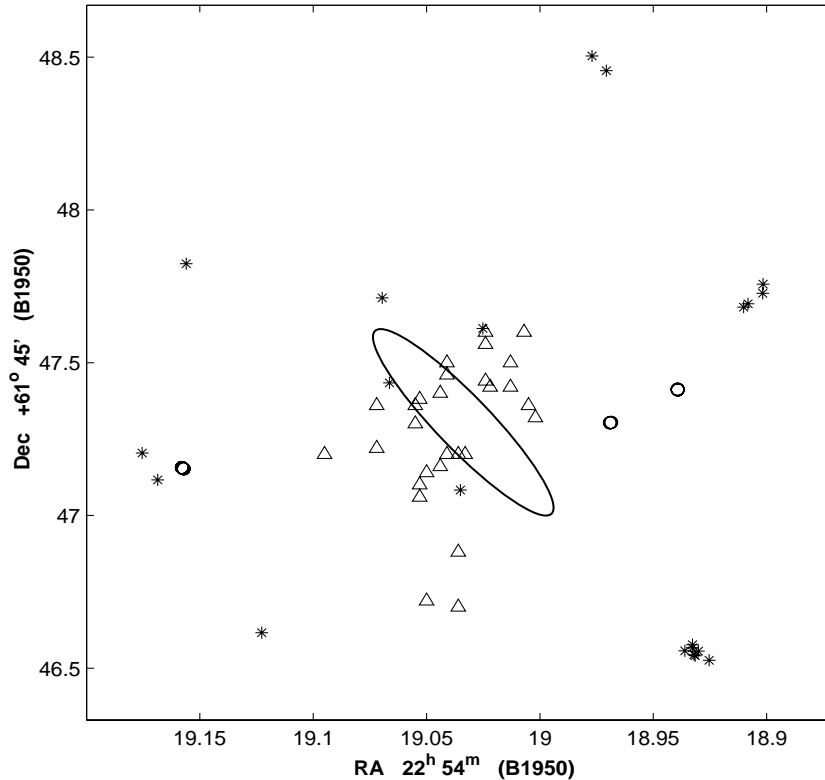


**Fig. 6.** Masers and radio jet in Cep A-HW2. The H<sub>2</sub>O (triangles), OH (stars) and 12.2 GHz CH<sub>3</sub>OH (circles) masers are shown. The ellipse represents the elongated radio continuum structure imaged by Torrelles et al. (1998). H<sub>2</sub>O, OH masers and radio jet positions are taken from Torrelles et al. (1998), Migenes et al. (1992). The positions of the radio source, H<sub>2</sub>O, OH masers are known to an accuracy of 100 to 300 mas

different stellar objects in G 9.62+0.20, the NIR emission in the *K*-band would appear before the UC H II phase, then the NIR emission would be progressively quenched as the H II region and the dusty envelope expand making the hot dust layer cool down. Two methanol maser sites in our sample, AFGL 5180 and S 255, are coincident with a NIR source that is clearly the signature of an embedded star. For instance, S 255 is located at the position of NIRS 3 which is a deeply embedded object with strong infrared excesses, powering an infrared jet and a CO outflow, and coincident with a weak radio continuum emission. The CH<sub>3</sub>OH maser site in S 255 is probably a massive protostar. The masers in AFGL 5180 coincide with NIRS 1 which has shaped a bipolar infrared reflection nebula, i.e. a dusty region associated with a bipolar outflow that reflects the radiation escaping from the central stellar object. Again, the methanol masers in AFGL 5180 mark the location of a very young stellar object. The masers in Mon R2 are also probably coincident with one of the three resolved NIR sources in IRS 3.

#### 4.3. Lonely methanol masers

Both S 269 and G 59.78+0.06 are associated with an IRAS source satisfying the colour criteria for UC H II regions. Nevertheless, Kurtz et al. (1994) did not detect any radio continuum emission toward these two sources. They

suggested that such sites were either low-mass star-forming regions or massive protostars. In the first case, no ionised region would be produced. In the second case, the ionised region would be so small and deeply embedded in the natal cocoon that no radio continuum could be detected. The idea that methanol masers without any radio continuum counterpart could arise from less massive stars than high-mass stars was first advanced by Phillips et al. (1998). This hypothesis could also explain the Keplerian sub-solar masses derived in Paper I for many methanol maser disk candidates. More recently, De Buizer et al. (2000) have imaged, in mid-infrared, the methanol maser sites studied by Phillips et al. (1998). In some cases, the position of methanol masers coincides with that of a compact mid-infrared emission, while no radio continuum emission at 8.6 GHz is seen near the maser position. De Buizer et al. argue that these methanol maser sites could be lower mass and non-ionising stars. However, the absence of radio continuum emission at 8.6 GHz do not necessarily prove that there is no ionised region associated with the methanol maser site. In the case of optically thick UC H II regions expected around massive protostars, the turn-over frequency, i.e. the frequency at which the free-free emission changes from an optically thick to an optically thin regime, could be higher than 8.6 GHz. For instance, Carral et al. (1997) found an ionised region near the cometary UC H II region G 75.78+0.34 with a

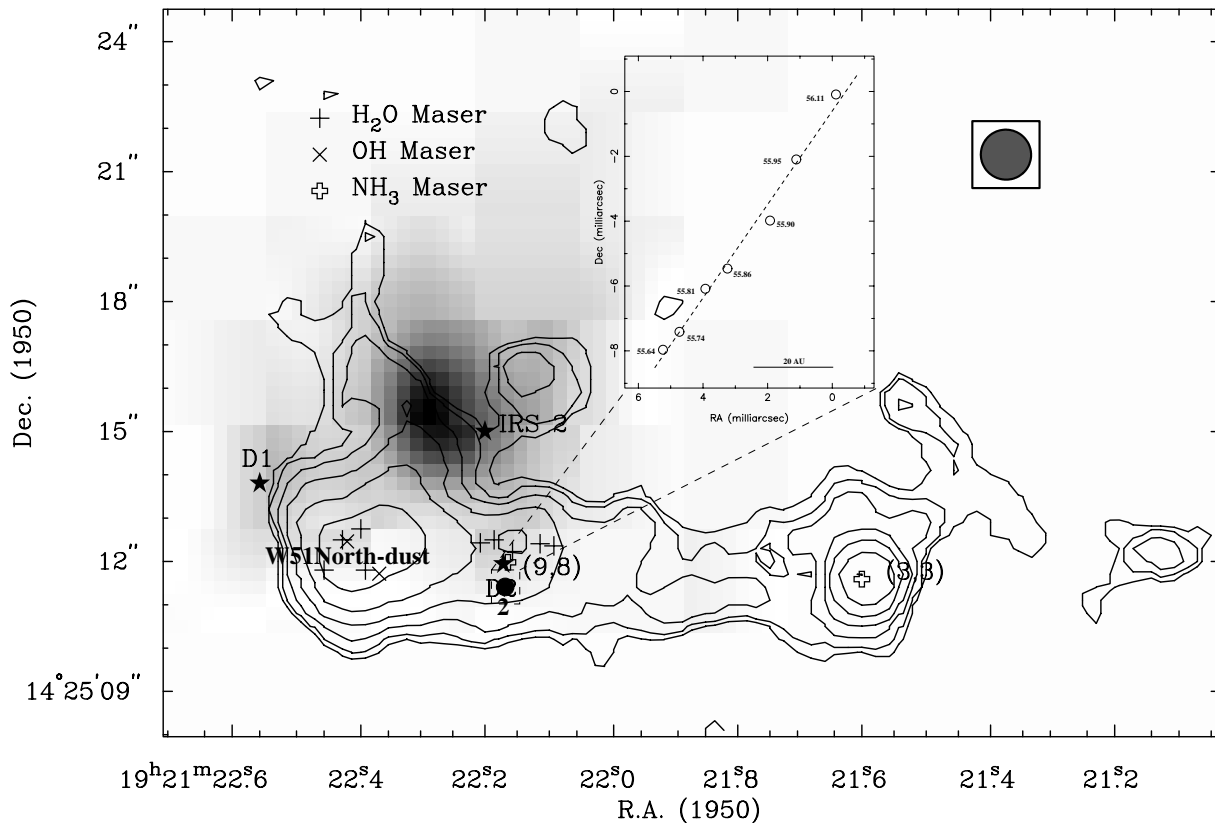


**Fig. 7.** Masers and  $\text{NH}_3$  thermal emission in W 51-North. Image adapted from Fig. 1 in Zhang et al. (1995) (reproduced by permission of the AAS). The contours represent the  $\text{NH}_3(3, 3)$  thermal emission overlaid on the 1.3 cm radio continuum (grey scale). The stars mark the positions of W51-D1, -D2 and -IRS 2. The black circle marks the position of the methanol maser site. The inset shows the methanol maser distribution at high resolution. The different masers are distributed along the elongated structure traced by ammonia. The positions of the radio source,  $\text{NH}_3$  thermal emission and masers,  $\text{H}_2\text{O}$ , OH masers are known to an accuracy of 100 to 300 mas

turn-over frequency of 15 GHz. Moreover, the emission from the deeply embedded ionised region is also detected at 43 GHz. Its position coincides with those of  $\text{H}_2\text{O}$  masers and it is located offset from the 5 GHz radio continuum peak emission that marks the position of the cometary UC H II region. Therefore, the lack of radio continuum emission associated with methanol masers could be explained by the hypothesis that the free-free emission is self-absorbed by the environment of massive protostars at low frequencies.

Methanol masers forming in shocked regions located far away from the young stellar object could also explain the case of the lonely masers. Such a situation is for example seen with  $\text{NH}_3$  masers in IRAS 20126+4106 by Zhang et al. (1999). While the present observations do not allow us to rule out the scenario of shock-pumped masers, models of Class II methanol masers, however, predict the formation of methanol masers in a warm dust environment near the young stellar object (e.g Cragg et al. 2001). In conclusion, since most of the methanol masers are clearly coincident with massive young stellar objects, it seems more likely that methanol masers without any radio continuum counterpart mark massive protostars rather than low-mass stars or distant shocked regions.

#### 4.4. Morphology of the methanol masers associated with outflows

An important question is where methanol masers originate; do they primarily trace disks or outflows or both? In Paper I, the large number of linear structures with linear velocity gradients was argued as evidence for a disk origin for many masers. We can try to test this hypothesis by looking at the geometrical relationships between the masers and larger scale structures such as outflows. In the sample discussed in this paper, seven methanol maser sites are located in the near (within 2 arcsec) vicinity of an outflow. In Table 2, the morphology of the maser components, as defined in Paper I, is compared to the nature of the neighbourhood of the maser sites. Within the seven sources coincident with outflows, four sources are *linear*, two are *simple* and one is *complex*.

Among these four linear sources, the lines of masers in NGC 7538 and AFGL 5180 are roughly perpendicular to the outflows (see PA in Table 2). However, other maser components in NGC 7538 are clearly distributed along the south part of the outflow (see Minier et al. 1998). Only one maser group in W 75N is aligned with an outflow (see PA in Table 2). Finally, the methanol masers in W 51 exhibit

**Table 2.** Comparison of the methanol maser positions to the positions of the tracers of embedded massive stellar objects such as ultra-compact H II regions (UC H II), outflows and hot molecular cores (HC). The morphology of the methanol masers is also given following the nomenclature in Paper I. The values in parenthesis in the second and third column give the position angles of the outflows and lines of masers, respectively. The fourth column is taken from Table 3, Paper I. It gives the length of the line of masers studied in Paper I. Column 5 gives the full extent of the maser component across the VLBI maps presented in Paper I. The exciting star type in Col. 6 is taken from publications referenced in the comments on each individual source. MP means massive protostar. In some cases, the nature of the YSO is unclear, i.e. star or protostar

Source	Coincident with (PA)	Morphology (PA)	Length (AU)	Total extent (AU)	Exciting star
IRAS 20126+4104	HC, Outflow	Simple	–	120	MP
NGC 7538	Outflow (0°)	Linear (110°)	280	1600	O9
AFGL 5180 (S252)	Outflow (130°)	Linear (70°)	240	240	MP(?)
G 31.28+0.06	–	Complex	780	2300	MP(?)
W 75N	Outflow (43°)	Linear (42°)	380	1000	OB
S 255	UC H II (?), Outflow (67°)	Complex	–	600	B1 or MP(?)
S 269	–	Linear	55	240	MP(?)
Mon R2	Unclear	Linear (50°)	130	130	?
G 9.62+0.20	UC H II	Linear	700, 350	700	B1
Cep A	Outflow (45°)	Simple	–	1200	B0.5
W 51	UC H II, Outflow (90°)	Linear (135°)	70	70	B0.5
G 59.78+0.06	–	Simple	–	–	MP(?)
G 29.95-0.02	HC	Linear	85	85	MP

a very small linear structure making an angle of 45° with the main direction of the elongated structure traced by NH<sub>3</sub> emission.

The masers in the *simple* source Cep A are not located exactly on the outflow, but they are offset from it by a few hundreds of AU. They might lie within a disk traced by the H<sub>2</sub>O masers.

In G 9.62+0.20-E, which is not associated with a known outflow source, the maser components delineate two parallel lines that are moving apart (Minier et al. 2001). The masers may trace an expanding ionising front or a wide-angle outflow.

Maser components associated with outflows, such as the southern blueshifted group in NGC 7538, may occur on larger scales because the outflows disturb the nearby environment of the protostars and contribute to the formation of a clumpy medium. Methanol masers could form within the dense and warm clumps. By comparing the map of the methanol masers with the high resolution map of the 22 GHz continuum in NGC 7538 (Gaume et al. 1995), it is striking that the methanol maser groups coincide with the resolved clumps in the uniformly weighted map (Fig. 3). The maser disk-like structure (black ellipse in Fig. 3) falls in between the northern and southern radio cores. It corresponds to the thin and denser strip bisecting the H66 $\alpha$  emission into two lobes, i.e. probably a disk around a central exciting star (see Gaume et al. for details). Note that the maser disk generates the main feature in the methanol spectrum (see Paper I, Fig. 1). The other components, corresponding to much lower flux densities, appear to coincide with the resolved clumps in

the 60 mas resolution image (right image in Fig. 3) located south of the disk. Also, the circular maser structure is seen projected onto the spherical radio component. This suggests that methanol masers form in two different environments, a disk and clumps in an outflow, as proposed by Sobolev et al. (1997). Following Sobolev’s model based on VLBI observations of 6.7 and 12.2 GHz methanol masers in W 3(OH), torsionally pumping masers should occur for  $n_{\text{H}}$  between  $3 \cdot 10^3$  and  $10^8 \text{ cm}^{-3}$ , high relative methanol abundance ( $X > 10^{-7}$ ) and warm dust ( $T_{\text{dust}} > 150 \text{ K}$ ). The maximum intensity is reached when  $n_{\text{H}} = 10^{7.5} \text{ cm}^{-3}$ ,  $X = 10^{-5}$  and  $T_{\text{dust}} = 150 \text{ K}$ . The methanol maser picture in NGC 7538-IRS 1 is consistent with Sobolev’s model: the most intense masers ( $>150 \text{ Jy}$ ) form in the dense and warm environment of the exciting star, while the weaker masers ( $<25 \text{ Jy}$ ) form in less dense ( $10^5 \text{ cm}^{-3}$ ) clumps further away. In the first case, the relatively warm temperature would enhance the abundance of methanol via evaporation of the icy dust mantles. The methanol is believed to be the second most abundant ice species in the environment of high-mass protostars (Dartois et al. 1999). In the case of masers occurring in clumpy molecular gas, the methanol could be injected into the molecular gas via evaporation driven by weak shocks (Hartquist et al. 1995). Such a heating mechanism would create sufficient methanol abundance despite lower temperature. The shocks would also be responsible for the formation of clumps.

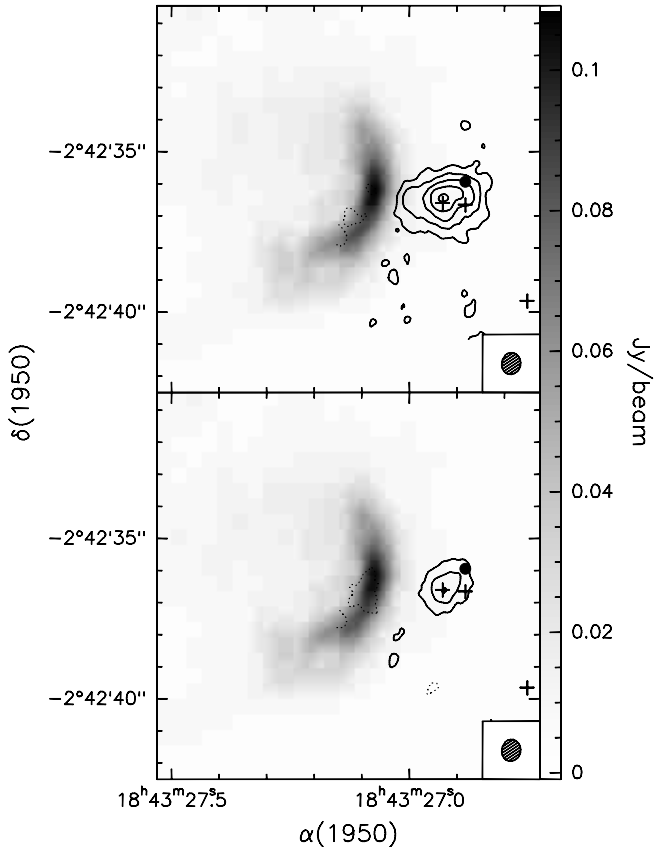


**Fig. 8.** Contour maps of G 29.95-0.02 in the  $\text{NH}_3(4,4)$  emission averaged over the main line (top) and over all the satellites (bottom) superimposed on the 1.3 cm continuum emission (grey scale) taken from Cesaroni et al. (1998) (reproduced with the permission of R. Cesaroni). The crosses mark the position of the water masers. The 12.2 GHz methanol masers (black circle) coincide with the  $\text{NH}_3$  core and with the  $\text{H}_2\text{O}$  masers. The positions of  $\text{NH}_3$  thermal emission and  $\text{H}_2\text{O}$  masers are known to an accuracy of 100 to 300 mas

#### 4.5. Morphology of the methanol masers in hot cores

The maser structures projected onto hot cores have much smaller total extent than those associated with outflows (see Table 2). However, the maser components are not located exactly at the centre of the hot core, i.e. onto the mm or  $\text{CH}_3\text{CN}$  peak emission; instead they lie offset from the exciting stellar object by  $\sim 1000$  AU. In Sect. 3.2, it has been suggested that the masers in IRAS 20126+4104 form in the interface between the  $\text{NH}_3$  disk and the outflow. This neutral layer of warm dust and gas ( $n_{\text{H}} = 10^7 \text{ cm}^{-3}$  as measured toward the  $\text{NH}_3$  core in G 29.96-0.02) could provide the FIR photons for pumping mechanism. Other possible sites such as the inner part of a disk or the termination of an outflow are physically unlikely because the ambient density conditions are not suitable for methanol masers. Indeed,  $\text{CH}_3\text{OH}$  masers cannot probably develop at the centre of the hot core because the gas is too dense and too hot. For instance, Cesaroni et al. (1997) derived a density of  $7 \times 10^8 \text{ cm}^{-3}$  and a temperature of 200 K toward the  $\text{CH}_3\text{CN}$  core (diameter of 1600 AU)

in IRAS 20126+4104. At such a density the absorption dominates and the methanol masers are quenched according to Sobolev's model. Conversely, methanol masers cannot form far away from a protostar within an outflow because the chemical abundance and densities are too low. Cesaroni et al. estimated the density of the ambient molecular gas surrounding IRAS 20126+4104. They probed the gas using CS and found  $n_{\text{H}} = 5 \times 10^5 \text{ cm}^{-3}$ , which is probably too low to produce a maser intensity of  $\sim 60$  Jy. Another factor to consider is the lifetime of hot cores which is only  $2 \times 10^3$  to  $5.7 \times 10^4$  years (see Kurtz et al. 2000). It requires  $10^4$ – $10^5$  years to obtain high methanol abundance via evaporation of the icy dust grain (van der Tak et al. 2000). Unlike the case of older objects such as NGC 7538, the methanol masers in hot cores have had no time to form far away from the protostar despite powerful outflows (e.g. IRAS 20126+4104) because the density is too low and the methanol abundance has not been enhanced at a sufficient level yet. Therefore the maser structure in hot cores remains small and compact near the exciting protostar. This scenario could also explain the short maser line in W 51, similar to the one in G 29.96-0.02, lying near a very recent hyper-compact H II region.

## 5. Conclusions

We have compared our VLBI maps of thirteen methanol masers with high resolution images at cm, mm and  $\mu\text{m}$  wavelengths of the associated star-forming regions published in the last ten years. Our main conclusions on different properties of the 6.7 and 12.2 GHz methanol masers, are as follows:

1. Eleven methanol maser sites out of thirteen studied cases do not coincide with any reported radio continuum emission that can be identified as a clear signature of a UC H II region. Only two sources, G 9.62+0.20 and W 51, coincide with a hyper-compact H II region;
2. When the methanol masers coincide in position with known infrared or mm continuum emission, they are located near (within 2000 AU) the exciting YSO. This YSO is either a massive protostar or a deeply embedded massive stellar object;
3. Seven methanol maser sites are located in the vicinity of an outflow and/or jet, i.e. within  $2000 \times 2000 \text{ AU}^2$  around the centre of an outflow. In one source (W 75N), some maser components are directly aligned along the direction of the jet. Three sources show linear structures roughly perpendicular to the outflows and with a linear velocity gradient along them (NGC 7538, AFGL 5180 and W 51). In three sources (IRAS 20126+4104, S 255 and Cep A), it is unclear whether the maser components are in a disk or in an outflow. These statistics suggest that the masers are associated with both outflows and protostellar disks;
4. The overall dimensions of the structures traced by the methanol masers may increase during the evolution of

the massive protostar. Our data suggest that they remain small and compact when associated with the hot core phase, and expand in sources associated with outflows. The methanol masers finally disappear when the UC H II region is well developed.

In summary, we have collected evidence suggesting that the methanol masers identify precursors of UC H II regions, and that the methanol masers are possibly the signature of massive protostars.

*Acknowledgements.* We are very grateful to Chris Phillips and Jim Caswell for communicating us the ATCA absolute positions of many sources. We also thank Mari Paz Miralles, Riccardo Cesaroni, Ralph Gaume, and Qizhou Zhang for giving us the permission to reproduce their figures.

## References

- Bachiller, R., & Tafalla, M. 1999, in *The Origin of Stars and Planetary Systems*, ed. C. J. Lada, & N. D. Kylafis (Kluwer Academic Publishers), 227
- Carral, P., Kurtz, S. E., Rodríguez, L. F., et al. 1997, *ApJ*, 486, L103
- Caswell, J. L., Vaile, R. A., Ellingsen, S. P., Whiteoak, J. B., & Norris, R. P. 1995, *MNRAS*, 272, 96
- Cesaroni, R., Felli, M., Testi, L., Walmsley, C. M., & Olmi, L. 1997, *A&A*, 325, 725
- Cesaroni, R., Hofner, P., Walmsley, C. M., & Churchwell, E. 1998, *A&A*, 331, 709
- Cesaroni, R., Felli, M., Jenness, T., et al. 1999, *A&A*, 345, 949
- Churchwell, E. 1999, in *The Origin of Stars and Planetary Systems*, ed. C. J. Lada, & N. D. Kylafis (Kluwer Academic Publishers), 515
- Codella, C., Testi, L., & Cesaroni, R. 1997, *A&A*, 325, 282
- Cragg, D. M., Sobolev, A. M., Ellingsen, S. P., et al. 2001, *MNRAS*, in press
- Davis, C. J., Moriarty-Schieven, G. H., Eislöffel, J., et al. 1998, *AJ*, 115, 1118
- Dartois, E., Schutte, W., Geballe, T. R., et al. 1999, *A&A*, 342, L32
- De Buizer, J. M., Piña, R. K., & Telesco, C. M., *ApJS*, 130, 437
- Ellingsen, S. P. 1996a, Ph.D. Thesis, University of Tasmania
- Ellingsen, S. P., Norris, R. P., & McCulloch, P. M. 1996b, *MNRAS*, 279, 101
- Gaume, R. A., Johnston, K. J., & Wilson, T. L. 1993, *ApJ*, 417, 645
- Gaume, R. A., Goss, W. M., Dickel, H. R., et al. 1995, *ApJ*, 438, 776
- Hartquist, T. W., Menten, K. M., Lepp, S., & Dalgarno, A. 1995, *MNRAS*, 272, 184
- Hofner, P., Kurtz, S., Churchwell, E., Walmsley, C. M., & Cesaroni, R. 1996, *ApJ*, 460, 359
- Hofner, P., Cesaroni, R., Rodríguez, L. F., & Martí, J. 1999, *A&A*, 345, L43
- Koresko, C. D., Beckwith, S., Ghez, A. M., et al. 1992, *AJ*, 105, 1481
- Kurtz, S., Churchwell, E., & Wood, D. O. S. 1994, *ApJS*, 91, 659
- Kurtz, S., Cesaroni, R., Churchwell, E., et al. 2000, in *Protostars and Planets IV*, ed. V. Mannings, A. P. Boss, & S. S. Russell (University of Arizona Press), 299
- Lada, E. A. 1999, in *The Origin of Stars and Planetary Systems*, ed. C. J. Lada, & N. D. Kylafis (Kluwer Academic Publishers), 441
- Menten, K. M. 1991, *ApJ*, 380, L75
- Migenes, V., Cohen, R. J., & Brebner, G. C. 1992, *MNRAS*, 254, 501
- Minier, V., Booth, R. S., & Conway, J. E. 1998, *A&A*, 336, L5
- Minier, V., Booth, R. S., & Conway, J. E. 1999, *NewAR*, 43, 569
- Minier, V., Booth, R. S., & Conway, J. E. 2000, *A&A*, 362, 1093, Paper I
- Minier, V., Booth, R. S., Ellingsen, S. P. et al. 2001, in *Proceedings of the 5th European VLBI Network Symposium*, ed. J. E. Conway, A. G. Polatidis, R. S. Booth, & Y. Pihlström, Chalmers Technical University, Gothenburg, Sweden, 179
- Miralles, M. P., Salas, L., Cruz-Gonzalez, I., & Kurtz, S. 1997, *ApJ*, 488, 479
- Moscadelli, L., Cesaroni, R., & Rioja, M. J. 2000, *A&A*, 360, 663
- Phillips, C. J., Norris, R. P., Ellingsen, S. P., & McCulloch, P. M. 1998, *MNRAS*, 300, 1131
- Rodríguez, L. F., Garay, G., Curiel, S., et al. 1994, *ApJ*, 430, L65
- Shu, F. H., Ruden, S. P., Lada, C. J., & Lizano, S. 1991, *ApJ*, 370, L31
- Snell, R. L., & Bally, J. 1986, *ApJ*, 303, 683
- Snell, R. L., Huang, Y.-L., Dickman, R. L., & Claussen, M. J. 1988, *ApJ*, 325, 853
- Sobolev, A. M., Cragg, D. M., & Godfrey, P. D. 1997, *A&A*, 324, 211
- Szymczak, M., Hrynek, G., & Kus, A. J. 2000, *A&AS*, 143, 269
- Tamura, M., Gatley, I., Joyce, R. R., et al. 1991, *ApJ*, 378, 611
- Testi, L., Felli, M., Persi, P., & Roth, M. 1998, *A&A*, 329, 233
- Torrelles, J. M., Gómez, J. F., Rodríguez, L. F., et al. 1996, *ApJ*, 457, L107
- Torrelles, J. M., Gómez, J. F., Rodríguez, L. F. et al. 1997, *ApJ*, 489, 744
- Torrelles, J. M., Gómez, J. F., & Garay, G. 1998, *ApJ*, 509, 262
- van der Tak, F. F. S., van Dishoeck, E. F., & Caselli, P. 2000, *A&A*, 361, 327
- Walsh, A. J., Hyland, A. R., Robinson, G., & Burton, M. G. 1997, *MNRAS*, 291, 261
- Walsh, A. J., Burton, M. G., Hyland, A. R., & Robinson, G. 1998, *MNRAS*, 301, 640
- Walsh, A. J., Burton, M. G., Hyland, A. R., & Robinson, G. 1999, *MNRAS*, 309, 905
- Wood, D. O. S., & Churchwell, E. 1989, *ApJ*, 340, 265
- Yao, Y., Hirata, N., Ishii, M., et al. 1997, *ApJ*, 490, 281
- Zhang, Q., & Ho, P. T. P. 1995, *ApJ*, 450, L63
- Zhang, Q., Ho, P. T. P., & Ohashi, N. 1998a, *ApJ*, 494, 636
- Zhang, Q., Hunter, T. R., & Sridharan, T. K. 1998b, *ApJ*, 505, L151
- Zhang, Q., Hunter, T. R., Sridharan, T. K., & Cesaroni, R. 1999, *ApJ*, 527, L117